Bluetooth Signal Attenuation Analysis in Human Body Tissue Analogues

MICHAEL J. CHRISTOE[1], **(Graduate Student Member, IEEE),**
JINHONG YUAN[2], **(Fellow, IEEE), ARON MICHAEL**[2], **(Member, IEEE),**
AND KOUROSH KALANTAR-ZADEH[1], **(Senior Member, IEEE)**

[1]School of Chemical Engineering, University of New South Wales, Sydney, NSW 2052, Australia
[2]School of Electrical Engineering and Telecommunications, University of New South Wales, Sydney, NSW 2052, Australia

Corresponding author: Kourosh Kalantar-Zadeh (k.kalantar-zadeh@unsw.edu.au)

ABSTRACT Wireless communications for ingestible and implantable medical device applications are integral for the embedded systems employed to these ends. The Bluetooth protocol is of major interest given its ubiquitous nature in consumer electronic devices. Here the effectiveness of Bluetooth in such applications is examined with a custom-designed Bluetooth system. The radio frequency (RF) attenuation testing was conducted in a variety of different media, including water, meat, ballistic gel, and fat. The RF signal attenuation was found to be the highest in meat and ballistic gel, less in water and least severe in fat. The measured distances at which signal integrity was still maintained provide necessary information for designing and implementing Bluetooth based medical devices and function as evidence for the feasibility of Bluetooth enabled systems for such communications.

INDEX TERMS Channel characterization and modeling, propagation, sensor networks, experimental and prototype results.

I. INTRODUCTION

Wireless medical devices that can be implanted or ingested are becoming more prevalent [1]–[12]. Many of these devices use proprietary radio protocols operating in industrial, scientific and medical (ISM) bands such as 433 MHz and 915 MHz [13], [14] or standardised radio protocols, specifically for medical use like MedRadio (formerly medical implant communication service (MICS)) and the wireless medical telemetry service (WMTS) [15]. However, since these radio protocols are not commonly implemented in consumer electronic devices such as smartphones, it is necessary for such devices to use intermediate transceivers to convert between protocols. Today it is common for smartphones to implement Wi-Fi, Bluetooth, and near-field communication (NFC) transceivers [16]–[18], but given the high power consumption of Wi-Fi and the short range of NFC [19], Bluetooth appears to be the best candidate for a direct point-to-point connection between a consumer electronic device and an ingestible or implantable electronic device. Recent

The associate editor coordinating the review of this manuscript and approving it for publication was Derek Abbott.

examples have also shown the viability of Bluetooth in medical devices [2], [20]. In addition, Bluetooth can offer versatility for internet of things (IoT) applications through direct connection to various common consumer devices such as smartphones, smartwatches and laptops, since this eliminates the need for the development of custom gateways that would be required for less common protocols [21]. Bluetooth can also be considered relatively safe, as the power output of Bluetooth transmitters is much lower than that of other consumer radio frequency (RF) transmitters such as those used in mobile phone networks [22] and is also well within the limits specified by the international commission on non-ionizing radiation protection (ICNIRP) [23]. However, given the absorption of 2.4 GHz radiation by human tissue and the relatively low transmission power of standard Bluetooth devices, there is cause for concern regarding whether the radio frequency attenuation in ingestible and implantable applications will be too great for Bluetooth to be feasible.

There are other pieces of literature that cover related topics but do not directly address the issue of Bluetooth feasibility in this application space. This paper [24] is a very comprehensive simulation of different digital human phantoms for

evaluating the link budgets of wireless implants around the body. However, it focuses on 402 MHz and 868 MHz. Another simulation paper [25] covered these two bands together with 2.4 GHz and is a good reference for acquiring data about RF propagation in applications where transmitter devices are located in the stomach. The outcomes from this can be used as a base for comparison with actual measurements. Some lab tested devices have been shown that operate at 865 MHz for use as 'self-sensing' radio frequency identification (RFID) sensors [26]. There are also other reports regarding propagation of waves through human tissue in other frequency ranges including within the 3–11 GHz range [27], [28]. While there are discussions about the use of near field magnetic induction (NFMI), which can offer better penetration and therefore improve signal integrity and reduce power consumption, the fact that it uses lower frequency bands results in severe limitations on data transmission rates in comparison to the common high frequency 2.4 GHz band [29].

In this paper, the suitability of Bluetooth for ingestible or implantable embedded systems applications is examined *via* RF attenuation testing through a selection of different media chosen for their suitability as human tissue analogues. A custom-made Bluetooth system is designed and implemented for carrying out the test with known communications protocol parameters. Section II describes the Bluetooth device used in the experiment. Section III documents the experimental setup. Section IV presents the experimental results and provides a detailed discussion of the results with comparison to data derived from other literature. The paper is concluded in section V.

II. BLUETOOTH SYSTEM

A prototype telecommunications system was developed. This consisted of a 15×40 mm printed circuit board (PCB) mounted with a Bluetooth system-on-chip (SoC) (Silicon Labs BGM11S), and a voltage regulator (Microchip MCP1810T-33I/J8A). The BGM11S module has an internal antenna which was used in this design. Fig. 1 shows the prototype PCB. The system receives power from a 3.3 V voltage regulator, which can step down an external power supply, such as a battery, of up to 5 V. The programmer interface is provided to allow for the reprogramming of the Bluetooth SoC while on the board.

The Bluetooth technology used here is Bluetooth low energy (BLE). The physical layer of BLE is defined in the Bluetooth standard specifications [30]. BLE uses a subset of the 2.4 GHz ISM band, from 2.4 GHz to 2.4835 GHz, subdivided into 40 channels with 1 MHz bandwidth. The maximum allowed transmitter output power is +10 dBm, though not all compliant devices are capable of this as they are designed with lower maximum output power in mind. The modulation scheme used is Gaussian frequency shift keying (GFSK) with a modulation index between 0.45 and 0.55.

The Bluetooth system, as with any implementation of the Bluetooth standard, periodically transmits advertising
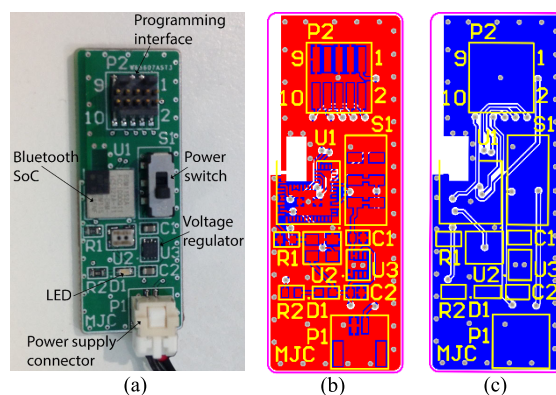

FIGURE 1. a) Photo of Bluetooth system PCB b) Top layer schematic of PCB c) Bottom layer schematic of PCB.

packets while it is unpaired. When these are received by other Bluetooth devices in range, the contents of the packet are passed up to the application layer of the software in the system, along with other information such as the received signal strength indicator (RSSI), which is measured by the Bluetooth transceiver upon reception of a packet. The RSSI is leveraged in these experiments to infer the relative attenuation of Bluetooth transmissions under different conditions.

III. BLUETOOTH RF ATTENUATION TESTS

RF attenuation testing was performed by placing the Bluetooth system in different media at various depths and then recording the RSSI as measured by a smartphone (Nokia 2.2, Bluetooth 4.2) outside the media. The media tested were water, ballistic gel (10% w/w gelatine in water), meat (beef) and fat (pork skin). A model of experimental set up is found in Fig. 2.a. Ballistic gel is a common material for simulating human tissue as previously reported [31]. Examples of the experimental setup for each media can be seen in Fig. 2.b-e. For the purposes of the radio attenuation tests, the Bluetooth system board was connected to a $3 \times$ AAA battery pack for power supply. The whole system was packaged in two airtight resealable bags to isolate the device from each medium it was placed in.

A. WATER

The system was taped to the bottom of a wooden rod which was dipped into a large plastic tub (approx. $280 \times 400 \times 250$ mm) filled with water and held in place by an adjustable stand. The height of the rod in the stand was incrementally adjusted to measure the RF attenuation at different depths with a smartphone (Nokia 2.2, Bluetooth 4.2) placed directly underneath the tub. The depth of the Bluetooth system for each signal strength measurement was measured using a ruler.

B. BALLISTIC GEL

Slices of ballistic gel were made by setting 1 L of 10% w/w gelatine powder in water mixture in containers that measured approx. 155×220 mm in the horizontal plane. A cavity was
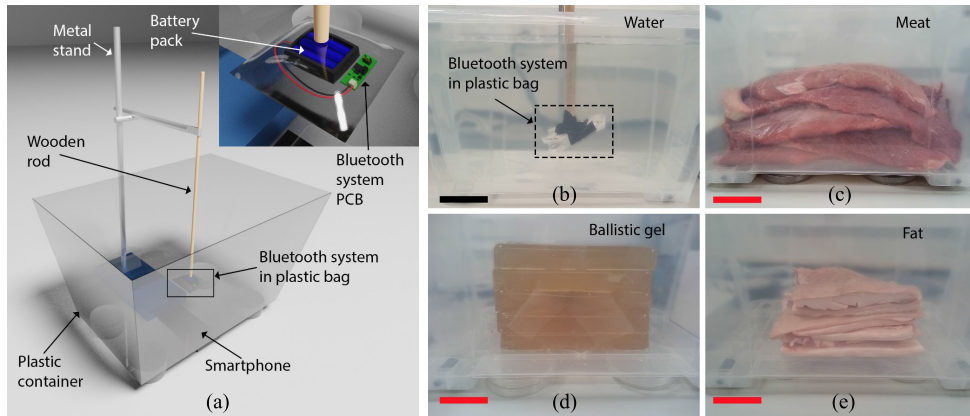
FIGURE 2. (a) Schematic diagram of RF attenuation experiment setup. b-e) Photos of RF attenuation experiment setup for b) Water c) Meat d) Ballistic gel e) Fat. Black scale bar = 80 mm, red scale bar = 70 mm.

cut out of the centre of one of the slices to place the Bluetooth system in and slices were incrementally added to the top and bottom of this slice in order to adjust the depth of the ballistic gel for each measurement. Like with the water test, the depth of the Bluetooth system was measured with a ruler and the signal strength measured by a smartphone directly under the tub containing the experiment.

C. MEAT
Large slices of beef were purchased from a local butcher. The Bluetooth system was placed between two slices of beef, with more slices incrementally added for each measurement. Method effectively identical to that of ballistic gel. Meat slices were on average approximately 210 mm × 350 mm.

D. FAT
Same as meat but with slices of pork skin purchased from butcher. Fat slices were on average approximately 150 mm × 250 mm.

Note on the dielectric properties of media used: it is important to consider that measurements can also be further fine-tuned. It is possible to refine a gel formula that has dielectric properties much closer to that of a specific human muscle tissue. However, the dielectric properties of muscle tissues vary from person to person due to age, gender, health, and many other parameters. It is therefore reasonable to use our ballistic gel as formulated here, which is an acceptable analogue to human tissues. Similarly, pork fat can be different from that of a human with respect to dielectric properties and moisture content. However, given the variation in the dielectric properties of human adipose tissue from person to person it is also acceptable to use pork fat as an analogue to human adipose tissue as an approximation.

IV. RESULTS AND DISCUSSION
Fig. 3 shows the attenuation of the Bluetooth signal in the different media tested at various depths. An approximation of the RF attenuation rate in each medium is also presented

in Table 1. RF attenuation is most severe in meat and ballistic gel, less severe in water and least severe in fat. The fact that the meat and ballistic gel data correlates so well appears to indicate that ballistic gel is a suitable analogue for muscle tissue. While further experimentation on fat was performed to attempt to obtain more data, it was found that the setup was insufficient due to the slices of pork skin being not wide enough to provide the tested thickness in all dimensions for the higher thickness tests.

TABLE 1. Bluetooth RF attenuation rate in multiple media as calculated from measurements, in comparison with theoretical RF attenuation rate for 2.4 GHz as derived from the permittivity of each medium [32], [33].

Medium	α_R [1] (dB/mm)	ε' [2]	ε'' [3]	κ [4] (S/m)	α_T [5] (dB/mm)
Meat	0.397	54.75 [34]	16.7 [34]	2.22	0.737
Ballistic gel	0.314	55.45 [35]	10.9	1.45 [35]	0.480
Water	0.287	78 [32]	7.8 [32]	1.04	0.259
Fat[6]	0.193	10.8 [36]	2.0	0.27 [36]	0.200

[1]RF attenuation rate for Bluetooth system
[2]Real part of relative dielectric permittivity
[3]Imaginary part of relative dielectric permittivity
[4]Conductivity
[5]Theoretical RF attenuation rate
[6]Average infiltrated

For tests in media other than fat, testing depth was limited by the effective receiver sensitivity of the Bluetooth devices in the system. RSSI readings of down to approx. −80 dBm were recorded, below which not all data packets were received in a given test. It should be noted that the Bluetooth low energy protocol uses Gaussian frequency shift keying (GFSK) modulation, which plays a role in improving the receiver sensitivity of the system [30].

Table 1 also presents the theoretical RF attenuation rate for each medium at 2.4 GHz as derived from the relative permittivity. The real (ε') and imaginary (ε'') parts of the relative permittivity of a medium can be used to calculate the loss tangent [32]:

$$\tan \delta = \frac{\varepsilon''}{\varepsilon'} \tag{1}$$
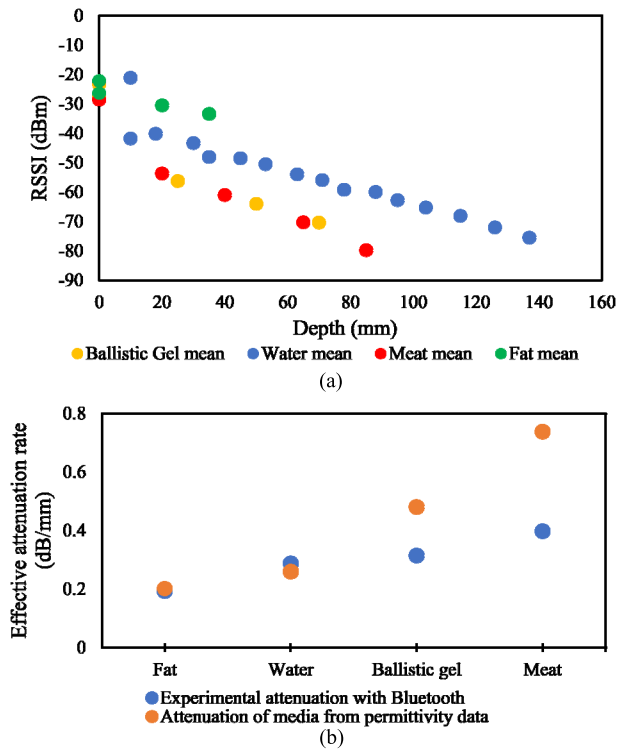
(a)

(b)

FIGURE 3. (a) Bluetooth RF attenuation in multiple media. Datapoints represent mean values of RSSI data collected from approx. 50 packets for each test. (b) RF attenuation rates for each media as measured from the Bluetooth attenuation experiment against the attenuation rates calculated from the permittivity of each media.

Relative permittivity is often reported in literature with the real component and the conductivity of the medium. In this case the imaginary part of the relative permittivity can be calculated as follows [32]:

$$\varepsilon'' = \frac{\kappa}{\omega \varepsilon_0} \qquad (2)$$

where κ is the conductivity of the medium, ω is the angular frequency of the RF radiation, and ε_0 is the permittivity of free space.

With the relative permittivity, loss tangent and the wavelength of the RF radiation in the medium of interest, it is possible to calculate the attenuation rate with the following [32]:

$$\alpha = \frac{27.3 \sqrt{\varepsilon_R} \tan \delta}{\lambda_0} \qquad (3)$$

where ε_R is the relative permittivity of the medium and λ_0 is the wavelength of the RF signal in the medium.

While the calculated theoretical attenuation rates for water and fat are quite similar to the attenuation rates obtained from the experimental data, the theoretical attenuation rates for meat and ballistic gel are relatively much higher. This means that the measured performance of the 2.4 GHz Bluetooth signal in meat and ballistic gel is better than what was predicated. This is due to the use of GFSK modulation by the Bluetooth protocol that mathematically increases the statistical probability of extracting the correct data from the
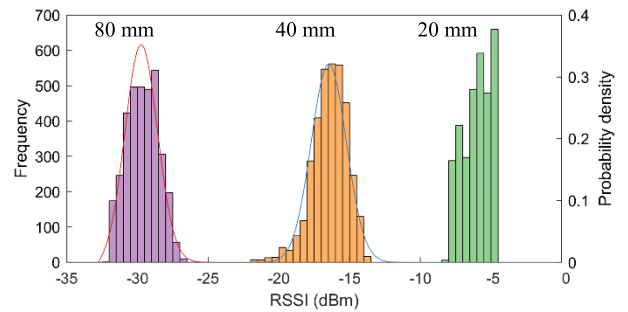

FIGURE 4. Probability distributions of RSSI at different depths in water. RSSI data have been shifted with reference to its value at 0 mm.

background noise [30]. This effect is more pronounced for gel and meat media as their physical signal attenuations are high and hence the direct extractions of the signals are not possible at relatively large distances.

Further tests were performed in water in order to obtain statistical distributions of RSSI for the received signal at different depths. Measurements in water were repeated to obtain approximately 3,000 samples at each depth. As can be seen in Fig. 4, histograms of the RSSI for the received data are presented for 3 distances of 20 mm, 40 mm, and 80 mm. The histogram of 20 mm does not show any specific distribution. However, when the distance increases, they are compared to Rician distributions [37]. Here, the Rician distribution[1] defines the probability of receiving a signal $p(x)$ with a power of x dBm, $(x \geq 0)$ as:

$$p(x) = I_0 \left(\frac{xs}{\sigma^2} \right) \frac{x}{\sigma^2} e^{-\left(\frac{x^2 + s^2}{2\sigma^2} \right)} \qquad (4)$$

where I_0 is the zero-order modified Bessel function of the first kind, s (non-centrality parameter) is the peak power of the line of sight (LOS) component, and σ^2 is the time-average power of the received radio signal. The distribution is described by the parameter $K = s^2/2\sigma^2$. For 80 mm the value of s is equal to 2.79 and $\sigma = 1.18$, which results in a K factor of 2.79, while for 40 mm, these values are $s = 5.64$ and $\sigma = 1.25$, resulting in a K factor of 10.02. Beyond 90 mm signal drop off was significant.

The increased performance in signal acquisition at longer distances in this system is due to the modulation scheme used. If no modulation is used, the path loss is directly proportional to the distance between the transmitter and the receiver. However, when the modulation scheme used by Bluetooth (GFSK) is used, the distribution of the received signal is approximated by (4), which has an increased probability of extracting the signal from the background noise. This is especially valuable when the attenuation of signal is high, such as in the gel and meat media as per Table 1.

It should be noted that in our work the RSSI data for the receiver in the phone was obtained using the ScanResult class of the Android application programming interface (API).

---

[1] As the histograms are plotted for RSSI in dBm, strictly speaking the RSSI is compared with log-Rician distributions.

Objects of this class are returned from running a Bluetooth low energy (BLE) scanner process which listens for BLE advertising packets in order to discover BLE devices that are in range of the phone. Objects of the ScanResult class contain an RSSI parameter which records the RSSI of the advertisement packet that the ScanResult object describes. Any lower level understanding of how the RSSI is obtained from the hardware cannot be determined from the documentation available as they are trade secrets for the chipset vendor Mediatek (no documentation was available for the phone's chipset beyond a brief product brochure) and the Android API is limited in its description (as also suggested by other researchers and users [38]). The BGM11S Bluetooth SoC used here has a maximum TX power output of +8 dBm. The mobile phone (Nokia 2.2) uses the Mediatek MT6761 Helio A22 chipset. The implementation of this API used in our work was through a free commercial app called "nRF Connect" from Nordic Semiconductor who also make a range of Bluetooth SoCs.

Given that the orientation of the Bluetooth module could have potentially influenced the RSSI readings recorded by the phone, further testing was performed in water for vertical and horizontal orientations of the Bluetooth device. The results of this can be found in Fig. 5, which shows that orientation appeared to have a negligible effect on the RSSI readings. An important aspect is the antenna-human body interaction along with antenna type and its orientation. Although we looked at the orientation, for specific antennas and designs this can be an issue. For instance, meandering pattern antennas, commonly used for capsules operating at 433 MHz, often have non-omnidirectional radiation patterns [39]–[41]. Such problems also can be an issue for antennas designed to operate at 2.4 GHz. However, available examples show that such antennas for 2.4 GHz are more omnidirectional [42]. Different types of patterns have been suggested for 2.4 GHz include axial mode helical, patch, angular ring patch, Yagi patch, dipole array, microstrip patch antennas [43], which should be fully investigated for ingestible or implantable applications regarding their radiation patterns.
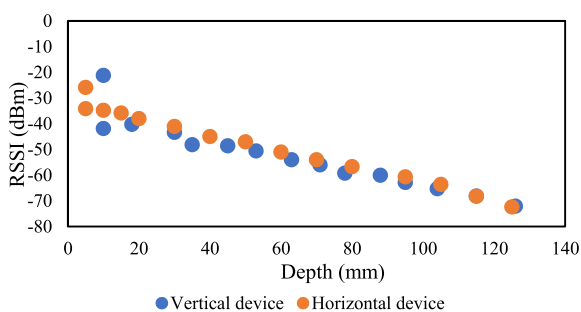

FIGURE 5. Bluetooth RF attenuation in water for device at different orientations. Datapoints represent mean values of RSSI data collected from approx. 50 packets for each test.

The results indicate that an implantable or ingestible device using Bluetooth for communication through the human body may be feasible, while the thickness of the body tissue should be considered for the possible loss of data. Given a lower limit of -80 dBm RSSI for successful packet transmission, the depth of muscle tissue that the system could transmit through was approximately up to 85 mm. This is not a particularly thick barrier, but it should be kept in mind that the path from a position inside the body to a position external to the human body does not only consist of muscle tissue but also fat, soft tissues and water, which appear to attenuate the 2.4 GHz signal at lower rates. It is conceivable that the total link budget could accommodate transmission through these materials over a typical distance from internal organs to air. While our measurements provide great information regarding the propagation and link budget for 2.4 GHz, the outcomes can become more comprehensive by adding multiple layers of body tissue structures together to make the outcomes closer to reality [44].

Another point of note is that this setup used Bluetooth 4.2 devices. More recent consumer devices (i.e. smartphones) typically implement Bluetooth 5, and Bluetooth SoCs implementing this version are now commonly available. Bluetooth 5 implements forward error correction (FEC) which can effectively increase the sensitivity of the receiver at the cost of channel capacity by adding in redundant bits. The improved sensitivity is advertised to be around up to 6 dB [45]. The improved sensitivity could significantly increase the feasibility of Bluetooth in ingestible applications.

As a final comment, we would like to add that typically in RF attenuation measurements single frequency transmission is considered. However, this work, relying on using modulated signal measurements, is a fully practical experiment that presents measurement results to show the viability of Bluetooth communications systems for ingestible and implantable applications. It is important to consider that this may not be applicable to other designs or protocols.

V. CONCLUSION

Measuring the RF signal attenuation of a Bluetooth device in different media analogous to human tissue has provided insight into the feasibility of Bluetooth for *in vivo* applications. The attenuation varies in different tissue types, with muscle tissue seemingly attenuating signals more than in reservoirs of water or fatty tissue. The orientation of a device as it moves through the body, for example through the digestive tract, appears to not affect RF signal attenuation for these devices. Communication could be demonstrated for reasonable depths of up to around 85 mm, which could be further improved with the introduction of FEC in Bluetooth 5. All in all, while testing in humans is required to confirm the feasibility of Bluetooth in these applications, for now it can be said that the use of Bluetooth for *in vivo* applications looks quite promising.

REFERENCES

[1] K. Kalantar-zadeh, N. Ha, J. Z. Ou, and K. J. Berean, "Ingestible sensors," *ACS Sensors*, vol. 2, no. 4, pp. 468–483, Apr. 2017, doi: 10.1021/acssensors.7b00045.

[2] A. D. Mickle, S. M. Won, K. N. Noh, J. Yoon, K. W. Meacham, Y. Xue, L. A. McIlvried, B. A. Copits, V. K. Samineni, K. E. Crawford, and D. H. Kim, "A wireless closed-loop system for optogenetic peripheral neuromodulation," *Nature*, vol. 565, no. 7739, pp. 361–365, Jan. 2019, doi: 10.1038/s41586-018-0823-6.

[3] M. S. Arefin, J.-M. Redoute, and M. R. Yuce, "Integration of low-power ASIC and MEMS sensors for monitoring gastrointestinal tract using a wireless capsule system," *IEEE J. Biomed. Health Informat.*, vol. 22, no. 1, pp. 87–97, Jan. 2018, doi: 10.1109/JBHI.2017.2690965.

[4] F. N. Alsunaydih, M. S. Arefin, J.-M. Redoute, and M. R. Yuce, "A navigation and pressure monitoring system toward autonomous wireless capsule endoscopy," *IEEE Sensors J.*, vol. 20, no. 14, pp. 8098–8107, Jul. 2020, doi: 10.1109/JSEN.2020.2979513.

[5] M. Rehan, I. Al-Bahadly, D. G. Thomas, and E. Avci, "Capsule robot for gut microbiota sampling using shape memory alloy spring," *Int. J. Med. Robot. Comput. Assist. Surg.*, vol. 16, no. 5, pp. 1–14, Oct. 2020, doi: 10.1002/rcs.2140.

[6] H. M. Bernety, H. Zhang, D. Schurig, and C. M. Furse, "Field focusing for implanted medical devices," *IEEE J. Electromagn., RF Microw. Med. Biol.*, vol. 4, no. 4, pp. 273–278, Dec. 2020, doi: 10.1109/JERM.2020.2983842.

[7] A. M. Chrysler, C. M. Furse, K. L. Hall, and Y. Chung, "Effect of material properties on a subdermal UHF RFID antenna," *IEEE J. Radio Freq. Identificat.*, vol. 1, no. 4, pp. 260–266, Dec. 2017, doi: 10.1109/JRFID.2018.2791919.

[8] J. Z. Ou, C. K. Yao, A. Rotbart, J. G. Muir, P. R. Gibson, and K. Kalantar-zadeh, "Human intestinal gas measurement systems: *In vitro* fermentation and gas capsules," *Trends Biotechnol.*, vol. 33, no. 4, pp. 208–213, Apr. 2015, doi: 10.1016/j.tibtech.2015.02.002.

[9] G. E. Banis, L. A. Beardslee, J. M. Stine, R. M. Sathyam, and R. Ghodssi, "Gastrointestinal targeted sampling and sensing via embedded packaging of integrated capsule system," *J. Microelectromech. Syst.*, vol. 28, no. 2, pp. 219–225, Apr. 2019, doi: 10.1109/JMEMS.2019.2897246.

[10] G. E. Banis, L. A. Beardslee, J. M. Stine, R. M. Sathyam, and R. Ghodssi, "Capacitive sensing of triglyceride film reactions: A proof-of-concept demonstration for sensing in simulated duodenal contents with gastrointestinal targeting capsule system," *Lab Chip*, vol. 20, no. 11, pp. 2020–2032, Jun. 2020, doi: 10.1039/D0LC00133C.

[11] L. A. Beardslee, G. E. Banis, S. Chu, S. Liu, A. A. Chapin, J. M. Stine, P. J. Pasricha, and R. Ghodssi, "Ingestible sensors and sensing systems for minimally invasive diagnosis and monitoring: The next frontier in minimally invasive screening," *ACS Sensors*, vol. 5, no. 4, pp. 891–910, Apr. 2020, doi: 10.1021/acssensors.9b02263.

[12] S. H. Daneshvar, M. Maymandi-Nejad, M. R. Yuce, and J.-M. Redoute, "A variable-capacitance energy harvester with miniaturized inductor targeting implantable devices," *IEEE Trans. Ind. Electron.*, early access, Jan. 14, 2021, doi: 10.1109/TIE.2021.3050392.

[13] K. Kalantar-Zadeh, K. J. Berean, N. Ha, A. F. Chrimes, K. Xu, D. Grando, J. Z. Ou, N. Pillai, J. L. Campbell, R. Brkljača, K. M. Taylor, R. E. Burgell, C. K. Yao, S. A. Ward, C. S. McSweeney, J. G. Muir, and P. R. Gibson, "A human pilot trial of ingestible electronic capsules capable of sensing different gases in the gut," *Nature Electron.*, vol. 1, no. 1, pp. 79–87, Jan. 2018, doi: 10.1038/s41928-017-0004-x.

[14] S. J. Seidman, P. S. Ruggera, R. G. Brockman, B. Lewis, and M. J. Shein, "Electromagnetic compatibility of pacemakers and implantable cardiac defibrillators exposed to RFID readers," *Int. J. Radio Freq. Identif. Technol. Appl.*, vol. 1, no. 3, pp. 237–246, 2007, doi: 10.1504/IJRFITA.2007.015848.

[15] *Radio Frequency Devices (Title 47, Chapter 1, Part 15)*, US Federal Commun. Commission, Washington, DC, USA, 2019.

[16] Apple Inc. *Iphone 11 Technical Specifications.* Accessed: Feb. 22, 2021. [Online]. Available: https://www.apple.com/au/iphone-11/specs/

[17] Samsung. *Galaxy S20 Specification.* Accessed: Feb. 22, 2021. [Online]. Available: https://www.samsung.com/au/smartphones/galaxy-s20/specs/

[18] Huawei Device Co. *Huawei P40 5G Smartphone Specifications.* Accessed: Feb. 22, 2021. [Online]. Available: https://consumer.huawei.com/au/phones/p40/specs/

[19] M. J. Christoe, J. Han, and K. Kalantar-Zadeh, "Telecommunications and data processing in flexible electronic systems," *Adv. Mater. Technol.*, vol. 5, no. 1, Jan. 2020, Art. no. 1900733, doi: 10.1002/admt.201900733.

[20] T. Lewis, "Elon Musk's pig-brain implant is still a long way from 'solving paralysis,'" *Sci. Amer.*, Sep. 2020. Accessed: Sep. 21, 2020. [Online]. Available: https://www.scientificamerican.com/article/elon-musks-pig-brain-implant-is-still-a-long-way-from-solving-paralysis/

[21] G. Xu, "IoT-assisted ECG monitoring framework with secure data transmission for health care applications," *IEEE Access*, vol. 8, pp. 74586–74594, 2020, doi: 10.1109/access.2020.2988059.

[22] Federal Communications Commission. *RF Safety FAQ.* Accessed: Oct. 2, 2020. [Online]. Available: https://www.fcc.gov/engineering-technology/electromagnetic-compatibility-division/radio-frequency-safety/faq/rf-safety

[23] G. Ziegelberger, R. Croft, M. Feychting, A. C. Green, A. Hirata, G. d'Inzeo, K. Jokela, S. Loughran, C. Marino, S. Miller, and G. Oftedal, "Guidelines for limiting exposure to electromagnetic fields (100 kHz to 300 GHz)," *Health Phys.*, vol. 118, no. 5, pp. 483–524, 2020, doi: 10.1097/HP.0000000000001210.

[24] A. Sani, A. Alomainy, and Y. Hao, "Numerical characterization and link budget evaluation of wireless implants considering different digital human phantoms," *IEEE Trans. Microw. Theory Techn.*, vol. 57, no. 10, pp. 2605–2613, Oct. 2009, doi: 10.1109/TMTT.2009.2029770.

[25] A. Alomainy and Y. Hao, "Modeling and characterization of biotelemetric radio channel from ingested implants considering organ contents," *IEEE Trans. Antennas Propag.*, vol. 57, no. 4, pp. 999–1005, Apr. 2009, doi: 10.1109/TAP.2009.2014531.

[26] V. Makarovaite, A. J. R. Hillier, S. J. Holder, C. W. Gourlay, and J. C. Batchelor, "Passive UHF RFID voice prosthesis mounted sensor for microbial growth detection," *IEEE J. Radio Freq. Identificat.*, vol. 4, no. 4, pp. 384–390, Dec. 2020, doi: 10.1109/JRFID.2020.3011900.

[27] N. Chahat, M. Zhadobov, R. Sauleau, and K. Ito, "A compact UWB antenna for on-body applications," *IEEE Trans. Antennas Propag.*, vol. 59, no. 4, pp. 1123–1131, Apr. 2011, doi: 10.1109/TAP.2011.2109361.

[28] A. Kara, "Human body shadowing variability in short-range indoor radio links at 3–11 GHz band," *Int. J. Electron.*, vol. 96, no. 2, pp. 205–211, Feb. 2009, doi: 10.1080/00207210802524302.

[29] A. Pal and K. Kant, "NFMI: Near field magnetic induction based communication," *Comput. Netw.*, vol. 181, Nov. 2020, Art. no. 107548, doi: 10.1016/j.comnet.2020.107548.

[30] *Bluetooth Core Specification v4.2*, Bluetooth Special Interest Group (SIG), Washington, DC, USA, Dec. 2014.

[31] L. Galluccio, S. Milardo, and E. Sciacca, "A feasibility analysis on the use of ultrasonic multihop communications for E-health applications," in *Proc. IEEE Int. Conf. Commun. (ICC)*, May 2017, pp. 1–6, doi: 10.1109/ICC.2017.7996896.

[32] M. Hallikainen, "Microwave dielectric properties of materials," in *Encyclopedia of Remote Sensing*, E. G. Njoku, Ed. New York, NY, USA: Springer, 2014, pp. 364–374.

[33] I. Y. Yanina, E. N. Lazareva, and V. V. Tuchin, "Refractive index of adipose tissue and lipid droplet measured in wide spectral and temperature ranges," *Appl. Opt.*, vol. 57, no. 17, pp. 4839–4848, Jun. 2018, doi: 10.1364/AO.57.004839.

[34] O. Sipahioglu, S. A. Barringer, and C. Bircan, "The dielectric properties of meats as a function of temperature and composition," *J. Microw. Power Electromagn. Energy*, vol. 38, no. 3, pp. 161–169, Jan. 2003, doi: 10.1080/08327823.2003.11688496.

[35] E. Porter, J. Fakhoury, R. Oprisor, M. Coates, and M. Popović, "Improved tissue phantoms for experimental validation of microwave breast cancer detection," in *Proc. 4th Eur. Conf. Antennas Propag.*, Apr. 2010, pp. 1–5.

[36] S. Gabriel, R. W. Lau, and C. Gabriel, "The dielectric properties of biological tissues: III. parametric models for the dielectric spectrum of tissues," *Phys. Med. Biol.*, vol. 41, no. 11, pp. 2271–2293, Nov. 1996, doi: 10.1088/0031-9155/41/11/003.

[37] G. Giorgetti, A. Cidronali, S. K. S. Gupta, and G. Manes, "Exploiting low-cost directional antennas in 2.4 GHz IEEE 802.15.4 wireless sensor networks," in *Proc. Eur. Conf. Wireless Technol.*, Oct. 2007, pp. 217–220, doi: 10.1109/ECWT.2007.4403985.

[38] J. Larsson, "Distance estimation and positioning based on Bluetooth low energy technology," M.S. thesis, School Inf. Commun. Tech., KTH Royal Inst. Tech., Stockholm, Sweden, 2015. [Online]. Available: https://urn.kb.se/resolve?urn=urn:nbn:se:kth:diva-174857

[39] A. Basir, M. Zada, Y. Cho, and H. Yoo, "A dual-circular-polarized endoscopic antenna with wideband characteristics and wireless biotelemetric link characterization," *IEEE Trans. Antennas Propag.*, vol. 68, no. 10, pp. 6953–6963, Oct. 2020, doi: 10.1109/TAP.2020.2998874.

[40] J. Wang, M. Leach, E. G. Lim, Z. Wang, R. Pei, and Y. Huang, "An implantable and conformal antenna for wireless capsule endoscopy," *IEEE Antennas Wireless Propag. Lett.*, vol. 17, no. 7, pp. 1153–1157, Jul. 2018, doi: 10.1109/LAWP.2018.2836392.

[41] M. S. Arefin, J.-M. Redoute, and M. R. Yuce, "Meandered conformai antenna for ISM-band ingestible capsule communication systems," in *Proc. 38th Annu. Int. Conf. IEEE Eng. Med. Biol. Soc. (EMBC)*, Aug. 2016, pp. 3031–3034, doi: 10.1109/EMBC.2016.7591368.

[42] J. J. Baek, S. W. Kim, and Y. T. Kim, "2.4 GHz wide-bandwidth inverted-F antenna for capsule endoscope," *Microw. Opt. Technol. Lett.*, vol. 62, no. 3, pp. 1275–1280, Mar. 2020, doi: 10.1002/mop.32134.

[43] C. Gouveia, C. Loss, P. Pinho, and J. Vieira, "Different antenna designs for non-contact vital signs measurement: A review," *Electronics*, vol. 8, no. 11, p. 1294, Nov. 2019. [Online]. Available: https://www.mdpi.com/2079-9292/8/11/1294

[44] S. Subramanian, T. Packirisamy, M. Mahalingam, S. Ramanathan, and L. Gopal, "Scattering coefficients and pathgain of a multilayer tissue structure using ABCD matrix method," *J. Ambient Intell. Hum. Comput.*, vol. 98, pp. 1–8, Jun. 2020, doi: 10.1007/s12652-020-02244-z.

[45] M. S. Henrik Snellman, J. Knaappila, and P. Rahikkala. *Bluetooth 5, Refined for the IoT*. [Online]. Available: https://www.silabs.com/whitepapers/bluetooth-5-refined-for-the-iot
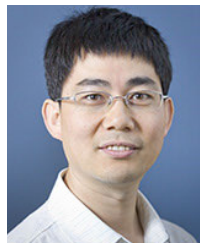
ARON MICHAEL (Member, IEEE) received the Ph.D. degree in electrical engineering from the University of New South Wales, Sydney, Australia, in 2007. He is currently a Lecturer with the School of Electrical Engineering and Telecommunication, University of New South Wales. He has published more than 80 scientific publications in his research areas. His current research interests include microelectromechanical systems-based optical switching, optical interconnects and chip cooling, piezoelectric actuators for micro-optics, evaporated thick silicon films, and silicon photonics for ultra-high sensitive displacement sensors.

MICHAEL J. CHRISTOE (Graduate Student Member, IEEE) received the B.Eng. degree in electrical and electronic from RMIT University, Australia, in 2018. He is currently pursuing the Ph.D. degree with the School of Chemical Engineering, University of New South Wales (UNSW), Australia. His research interests include the implementation of embedded systems for small, low power, wireless sensor applications, such as gas sensing for biomedical diagnostics, as well as using field programmable gate arrays (FPGAs) for embedded applications requiring highly efficient computation.

JINHONG YUAN (Fellow, IEEE) joined the School of Electrical Engineering and Telecommunications, University of New South Wales, Sydney, Australia, in 2000, where he is currently a Professor and the Head of Telecommunication Group. He has published two books, five book chapters, over 300 articles in telecommunications journals and conference proceedings, and 50 industrial reports. His current research interests include error control coding and information theory, communication theory, and wireless communications. He served as the IEEE NSW Chapter Chair for Joint Communications/Signal Processions/Ocean Engineering Chapter, from 2011 to 2014. He served as an Associate Editor for the IEEE Transactions on Communications, from 2012 to 2017. He is currently serving as an Associate Editor for the IEEE Transactions on Wireless Communications.

KOUROSH KALANTAR-ZADEH (Senior Member, IEEE) is a Professor of chemical engineering with the University of New South Wales (UNSW), Sydney, Australia. He is one of the Australian Research Council (ARC) Laureate Fellows of 2018. He is involved in research in the fields of materials sciences, electronics, and transducers. He has coauthored of over 450 scientific articles and books. He is also a member of the Editorial Board of journals, including *American Chemical Society (ACS) Sensors*, *ACS Applied Nano Materials*, *Advanced Materials Technologies*, *Nanoscale*, and *ACS Nano*. He has received many international awards including, IEEE Sensor Council Achievement, in 2017, ACS Advances in Measurement Science Lectureship Awards, in 2018, and Robert Boyle Prize for Analytical Science, in 2020, Royal Society of Chemistry (RSC), U.K. His name has also appeared in the Clarivate Analytics most highly cited list, since 2018.

● ● ●